Available online at www.sciencedirect.com
SCIENCE DIRECT®
Journal of Sound and Vibration 287 (2005) 667–682
JOURNAL OF SOUND AND VIBRATION
www.elsevier.com/locate/jsvi

A variable stiffness device selection and design tool for lightly damped structures ☆

M.F. Winthrop[a,*], W.P. Baker[b], R.G. Cobb[a]

[a] *Department of Aeronautics and Astronautics, Air Force Institute of Technology, 2950 Hobson Way, Wright-Patterson AFB, OH 45433, USA*
[b] *Department of Mathematics and Statistics, Air Force Institute of Technology, 2950 Hobson Way, Wright-Patterson AFB, OH 45433, USA*

Received 29 January 2004; received in revised form 13 September 2004; accepted 19 November 2004
Available online 1 February 2005

Abstract

Due to the wide variety of types and capabilities of variable stiffness devices, selecting a variable stiffness device for vibration control of a structure can be difficult. A method for selecting and understanding the performance of variable stiffness devices was developed. First, a parameter for roughly comparing variable stiffness devices was identified using the literature. Next, variable stiffness devices in the literature were summarized and compared by their ability to change stiffness. A single-degree-of-freedom variable stiffness vibration suppression problem was solved in an exact implicit form using the variable stiffness comparison parameter. The exact solution was used to create an approximate solution directly linking past variable stiffness approximations to the exact solution in a systematic way. The result is an engineering design tool that can be used in the design of structures with variable stiffness devices.
© 2004 Elsevier Ltd. All rights reserved.

☆ The views expressed in this article are those of the authors and do not reflect the official policy or position of the United States Air Force, the Department of Defense, or the US Government.

*Corresponding author. Tel.: +1 937 255 6565/4442; fax: +1 937 656 7621.
E-mail address: michael.winthrop@afit.edu (M.F. Winthrop).

0022-460X/$ - see front matter © 2004 Elsevier Ltd. All rights reserved.
doi:10.1016/j.jsv.2004.11.022

1. Introduction

Variable stiffness concepts have been widely studied in the literature and extensively reviewed for a variety of vibration control applications [1,2]. Numerous control laws have been proposed, such as discontinuous "bang-bang" control [3–5] and continuous control [4,6]. Additionally, a bewildering number of variable stiffness devices have been tested in the last decade.

Choosing a variable stiffness device for use in a structure requires some method of comparing the performance of various systems. This implies choosing a performance metric and then linking the metric to performance of a system. Achieving this goal can be quite difficult since real variable stiffness devices are nonlinear, differ significantly from each other, and are often controlled with nonlinear control laws.

This article makes several contributions. First, it briefly summarizes various variable stiffness devices and compares their ability to change stiffness by reviewing the literature. Second, it provides a rough comparison of the performance of different variable stiffness devices using a simple single-degree-of-freedom (sdof) model solved both exactly and approximately. A simple heuristic on–off control law commonly discussed in the literature is used. Third, it confirms past results in the literature by directly linking them to the exact solution. Finally, it provides an engineering tool for use in designing systems with variable stiffness devices.

2. Variable stiffness devices

Over the last decade, variable stiffness devices have been created using smart materials or through mechanical means. Recent work has focused on using smart materials. In a survey of the literature, variable stiffness devices were typically constructed from shape memory alloys (SMAs), piezoelectrics, and magnetorheological elastomers.

When reported, researchers often document the maximum and minimum natural frequencies achieved by the devices they studied, or they report the maximum and minimum stiffness of their device. Since actuating these devices does not change the mass of the system, the change in natural frequency, neglecting damping, can be used to calculate a device characterization parameter α. That is,

$$\alpha = \left(\frac{\omega^*_{\min}}{\omega^*_{\max}}\right)^2, \tag{1}$$

where $\omega^*_{\max}$ is the highest frequency attained by a device in a system and $\omega^*_{\min}$ is the lowest frequency attained. Alternatively, many researchers document the minimum and maximum stiffness values, denoted as k^*_0 and k^*_1, respectively. A second parameter ε is then defined as the ratio

$$\varepsilon = \frac{k^*_1 - k^*_0}{k^*_1 + k^*_0}. \tag{2}$$

The relation between these two parameters is easily seen as

$$\varepsilon = \frac{1-\alpha}{1+\alpha} \tag{3}$$

and thus

$$\alpha = \frac{k_0^*}{k_1^*}. \tag{4}$$

Note that $0 \leqslant \varepsilon < 1$ and $0 < \alpha \leqslant 1$. The parameter ε is a physical measure of the maximum variation of a variable stiffness device, while α is the variable stiffness ratio of a device.

As will be shown, a wide range of variable stiffness devices are available to the designer and thus a design tool for determining the achievable performance for each device is desired. In quantifying achievable performance, it will be assumed that these devices have the ability to respond quickly enough to be usable in real physical systems. The sections that follow briefly summarize how selected variable stiffness devices work and identify relevant data used to calculate α.

2.1. Shape memory alloys

SMAs are metal alloys that recover otherwise permanent strains when heated. SMAs have two properties which have been exploited for use in vibration control called the shape memory effect (SME) and the pseudoelasticity effect (PE). The SME occurs when a SMA in martensitic form is deformed by a load and then heated to austenitic form where it recovers its original shape. The PE occurs when a load is applied to an SMA in austenitic form, which under proper conditions can induce a phase change to martensitic form. When the load is released, the material is transformed back to austenitic form and recovers its original shape [7].

The PE has been studied as a replacement for softening springs in an isolator to decouple displacement and resonant frequency of the system [8,9]. While this is a variable stiffness concept, the control method typically employed is not simple on–off control as considered herein and thus PE devices are not further discussed.

The SME has been used to create isolators with fast response rates [10]. It has also been used to create tunable vibration absorbers. In one article, Williams et al. used three SMAs and steel wires configured as cantilever beams with a concentrated mass at the end to create a vibration absorber. The reported change in natural frequency was $\omega_{\min}/\omega_{\max} = \frac{1}{1.73}$, resulting in $\alpha = 0.33$ [11].

2.2. Magnetorheological elastomers

Magnetorheological elastomers (MREs) are solid polymers with dispersed polarizable particles. Application of a magnetic field to the MRE causes a change in stiffness. The elastomer is cured in a magnetic field, causing the magnetic particles to align in chains and remain aligned after the magnetic field is removed [12,13].

Zhou experimented with an MRE in a sdof system. He studied a device made of silicone rubber and containing 27% carbonyl iron particles. He experimentally determined the change in natural frequency and fitted his data to a polynomial. Zhou found he could vary the natural frequency of his system from 1397.6 to 1773.5 radians/s or $\alpha = 0.62$ [14].

In another experiment, Albanese and Cunefare tested silicone mixed with several different percentages of iron particle concentrations. They concluded that at 35% iron content, as much as a 400% change in frequency could be made by applying a magnetic field. In their conference

briefing, they concluded 30% iron content could cause a nearly 900% change in frequency. Their results are reported in terms of $\alpha^{-1/2}$ or, equivalently, they tested several devices in the range $0.11 \leqslant \alpha \leqslant 0.91$ [15,16].

2.3. Piezoelectrics

Stiffness of piezoelectrics can be varied by connecting them to a capacitive shunt circuit. This and other methods of shunting piezoelectrics for vibration control were reviewed by Lesieutre [17]. A simple method of varying the stiffness of piezoelectric devices is to switch it between open and closed circuit conditions. This has the effect of changing the electrical capacitance of the piezoelectric device and varies the stiffness between its highest and lowest stiffness values. Richard et al. experimented with this method and found superior performance as compared to a resistively shunted nonswitching system [18].

Corr and Clark have also experimented with this concept. For their setup, they concluded this method provided only small changes in stiffness and was not as effective as other shunt circuits with associated control laws. Other shunt circuits experimented with include pure resistor and resistor/inductor shunt circuits [19,20].

In an earlier paper, Clark analyzed effective beam stiffness in the case of a piezoelectric bonded to a cantilever. As the ratio of beam to piezoelectric patch thickness decreased, the open circuit to short circuit stiffness ratio or α^{-1} was found to increase to a maximum value approaching 2.0. That is, $\alpha \to \frac{1}{2}$ [21].

Varying stiffness has been used to tune vibration absorbers when the resonant frequency varies. Davis and Lesieutre created and demonstrated a tunable vibration absorber that tracked a disturbance frequency. The piezoelectric stiffness element was actively tuned using a shunt circuit ladder of capacitors allowing various discrete levels of capacitance to be chosen. Davis and Lesieutre were able to vary the natural frequency of their system by almost 7.5% over a range of 313–338 Hz [22]. This translates to an α of 0.86.

More recently, Ramaratnam et al. proposed using piezoelectrics for robotic applications. They simulated both open and closed switching and the use of capacitive shunt circuits to minimize the tip deflection of a translational flexible beam. Both methods achieved similar results. The capacitive shunt method allowed a more gradual change in stiffness than the open/closed switching method. Their predicted equivalent stiffness for the capacitive method translates to an α of approximately 0.045. Future experimental work is planned [23].

2.4. Other devices

Other methods of varying stiffness have been explored. One approach is to place a magnetorheological fluid (MRF) damper in series with a spring, which is then placed in parallel with another spring, creating a three-parameter isolator. Varying the MRF damping then changes the apparent stiffness of the isolator [24,25].

Two mechanical concepts for varying stiffness have been discussed in the literature. One concept is a vibration absorber that consists of a mass attached to a helical spring with a spring collar dividing the spring into two parts. The spring collar isolates part of the spring from the rest of the absorber and the number of coils used in the absorber can be changed by rotating the spring

[26]. Another concept is to connect two leaf springs in opposition to each other and use a stepper motor to increase the separation distance between the two springs. In this concept, the authors report a change of stiffness of $\alpha^{-1} = 62$ in a nonlinear range and $\alpha^{-1} = 45$ in an approximately linear range. The linear range where $\alpha = \frac{1}{45} = 0.02$ corresponds to a value for ε very close to its largest possible value [27].

2.5. Summary

Table 1 summarizes the results of these calculations for some proposed hardware values for ε and α found in the literature in order of reported ability to change stiffness from highest to lowest. These devices offer a wide range of choices for the control system designer, with a potential wide range of achievable performance. An analytical design tool is needed to help quantify the performance results from a particular hardware choice. In the following sections, an analytical solution of a well-known simplified model is obtained, and then used in the development of quantifiable design guides.

3. Variable stiffness model

A general sdof suppression problem has been considered by Leitmann [3] as

$$m^*\ddot{x}^* + c^*(v)\dot{x}^* + k^*(u)x^* = Q^*. \tag{5}$$

The function $Q^* = Q^*(t^*)$ is the disturbance to the system. The "*" notation identifies the variable as a dimensional variable. Variables without the "*" notation are nondimensional variables. The parameters $v \in [-1, 1]$ and $u \in [-1, 1]$ are control parameters that instantaneously change the stiffness and damping of the system. The stiffness $k^*(u)$ is defined as

$$k^*(u) = \tfrac{1}{2}[(k_0^* + k_1^*) + (k_1^* - k_0^*)u], \tag{6}$$

Table 1
Parameter values for proposed variable stiffness devices in the literature

Source	Year	Device	α	ε
Albanese and Cuefare [16]	2003	MRE 30% Fe	0.01	0.98
Walsh and Lamancusa [27]	1992	Leaf Spring	0.02	0.96
Albanese and Cuefare [15,16]	2003	MRE 35% Fe	0.05	0.91
Albanese and Cuefare [15,16]	2003	MRE 25% Fe	0.11	0.80
Albanese and Cuefare [15,16]	2003	MRE 40% Fe	0.19	0.68
Albanese and Cuefare [15,16]	2003	MRE 10% Fe	0.31	0.53
Williams, Chiu, and Bernhard [11]	2002	SMA	0.33	0.50
Albanese and Cuefare [15,16]	2003	MRE 50% Fe	0.35	0.49
Clark [21]	2000	Piezoelectric Patch on Cantilever (On-Off)	0.50	0.33
Zhou [14]	2003	MRE 27% Fe	0.62	0.23
Albanese and Cuefare [15,16]	2003	MRE 0%Fe	0.83	0.10
Ramaratnam, Jalili, and Grier [23]	2003	Piezoelectric (Capactive Shunt)	0.91	0.05
Davis and Lesieutre [22]	2000	Piezoelectric (Capactive Shunt)	0.93	0.04

where k_1^* and k_0^* are both positive and are the maximum and minimum stiffness achievable for the device, respectively. The damping function $c^*(v)$ is defined in a similar manner as Eq. (6).

Leitmann [3] develops a variable stiffness control law using an energy argument as

$$u = \operatorname{sgn}(x^*\dot{x}^*) = \begin{cases} 1 & \text{if } x^*\dot{x}^* > 0, \\ 0 & \text{if } x^*\dot{x}^* = 0, \\ -1 & \text{if } x^*\dot{x}^* < 0, \end{cases} \tag{7}$$

where sgn represents the sign or signum function. Leitmann concludes variable damping should always be maximum in the sdof suppression problem, so variable damping is not considered herein [3]. In the current effort, damping is assumed to be negligible (i.e. $c^* = 0$). Various versions of Eq. (5) have been considered by other authors [4,5]. For example, Douay and Hagood [4] considered the equivalent system

$$m^*\ddot{x}^* + (k^* + \tilde{k}^* u)x^* = 0. \tag{8}$$

With the change of variables

$$\tilde{k}^* = \frac{k_1^* - k_0^*}{2}, \tag{9}$$

$$k^* = \frac{k_1^* + k_0^*}{2}, \tag{10}$$

and

$$Q^* = 0, \tag{11}$$

Eqs. (5) and (8) are equivalent. The definitions of $\tilde{k}^*$ and k^* will be carried through into the results to simplify comparisons with the literature.

4. Problem statement in non-dimensional form

Of interest to the control designer is how performance is affected by choice of the variable stiffness hardware. For the undamped case, combining Eqs. (5) and (6) results in

$$m^*\ddot{x}^* + \tfrac{1}{2}[(k_1^* + k_0^*) + (k_1^* - k_0^*)\operatorname{sgn}(x^*\dot{x}^*)]x^* = 0, \tag{12}$$

with two sets of initial conditions. The first set is

$$x^*(0) = x_0^*, \quad \dot{x}^*(0) = 0 \tag{13}$$

and the second set is

$$x^*(0) = 0, \quad \dot{x}^*(0) = \dot{x}_0^*. \tag{14}$$

Eq. (12) can be nondimensionalized by defining the nominal natural frequency as

$$\omega_0^* = \sqrt{\frac{k_0^* + k_1^*}{2m^*}}, \tag{15}$$

and by defining a reference length, such that the nonzero initial condition will become unity. For the initial displacement problem defined by Eq. (13), use

$$L^* = x_0^*. \tag{16}$$

For the nonzero initial velocity, corresponding to Eq. (14), use

$$L^* = \frac{\dot{x}_0^*}{\omega_0^*}. \tag{17}$$

For both cases, time can be scaled to be

$$t = t^* \omega_0^* \tag{18}$$

and displacement can be scaled to be

$$x = \frac{x^*}{L^*}. \tag{19}$$

Note that L^* cannot equal zero since Eq. (19) becomes invalid. However, $L^* = 0$ implies no initial disturbance to the system, resulting in the trivial solution. In nondimensional form, Eq. (12) can then be rewritten as

$$\ddot{x} + x + \varepsilon \operatorname{sgn}(x\dot{x})x = 0, \tag{20}$$

with ε and α as previously defined,

$$\varepsilon = \frac{k_1^* - k_0^*}{k_1^* + k_0^*} = \frac{1-\alpha}{1+\alpha} = \frac{\tilde{k}^*}{k^*} \tag{21}$$

or in terms of α yields

$$\alpha = \frac{k_0^*}{k_1^*} = \frac{1-\varepsilon}{1+\varepsilon} = \frac{k^* - \tilde{k}^*}{k^* + \tilde{k}^*}. \tag{22}$$

It will be shown that ε or α are convenient variables for comparing the performance capabilities of variable stiffness devices.

5. Results

To solve Eq. (12), an implicit solution technique was developed using a perturbation technique on the piecewise linear solution. The full derivation of this technique is contained in the appendices, and only the results are presented below.

5.1. The exact solution

Appendix A contains the derivation of the exact implicit solution to Eq. (20) for the initial conditions

$$x(0) = 1, \quad \dot{x}(0) = 0, \tag{23}$$

while Appendix B provides an approximate explicit solution based on the exact implicit solution. Using the initial conditions of Eq. (23), the exact solution was found to be of the form

$$x(t) = a(\phi)\cos(t(\phi)). \tag{24}$$

By first defining the terms

$$n(\phi) = \text{floor}\left(\frac{2\phi}{\pi}\right) \tag{25}$$

and

$$J_k(\varepsilon) = \sqrt{\frac{2-\varepsilon[(-1)^k+1]}{2-\varepsilon[(-1)^k-1]}}, \tag{26}$$

where floor $(\bullet)$ rounds down to the nearest integer and $k = 0, 1, 2, \ldots$, the implicit time and amplitude are given by

$$t_d(\phi) = \begin{cases} \frac{1}{\sqrt{1-\varepsilon}}\tan^{-1}[\frac{1}{\sqrt{1-\varepsilon}}\tan(\phi)] & \text{if } 0 \leqslant \phi \leqslant \frac{\pi}{2}, \\ \frac{\pi}{2}\sum_{k=0}^{n-1}\frac{1}{\sqrt{1-(-1)^k\varepsilon}} + \frac{1}{\sqrt{1-(-1)^n\varepsilon}}\tan^{-1}(\frac{1}{J_n(\varepsilon)}\tan(\phi - \frac{n\pi}{2})) & \text{otherwise} \end{cases} \tag{27}$$

and

$$a_d(\phi) = \begin{cases} \sqrt{\frac{1-\varepsilon}{1-\varepsilon\cos^2\phi}} & \text{if } 0 \leqslant \phi \leqslant \frac{\pi}{2}, \\ \sqrt{\frac{2-\varepsilon[(-1)^n+1]}{2(1-\varepsilon(-1)^n\cos^2(\phi))}}\prod_{k=0}^{n-1} J_k(\varepsilon) & \text{otherwise.} \end{cases} \tag{28}$$

For the initial velocity condition,

$$x(0) = 0, \quad \dot{x}(0) = 1, \tag{29}$$

Eqs. (24)–(26) still apply, but the time and amplitude is given as

$$t_v(\phi) = \begin{cases} \frac{1}{\sqrt{1+\varepsilon}}\tan^{-1}\left[\frac{1}{\sqrt{1+\varepsilon}}\tan(\phi) + \frac{\pi}{2}\right] & \text{if } -\frac{\pi}{2} \leqslant \phi \leqslant 0, \\ \frac{\pi}{2}\sum_{k=-1}^{n-1}\frac{1}{\sqrt{1-(-1)^k\varepsilon}} + \frac{1}{\sqrt{1-(-1)^n\varepsilon}}\tan^{-1}\left(\frac{1}{J_n(\varepsilon)}\tan\left(\phi - \frac{n\pi}{2}\right)\right) & \text{otherwise} \end{cases} \tag{30}$$

and

$$a_v(\phi) = \begin{cases} \frac{1}{\sqrt{1+\varepsilon\cos^2\phi}} & \text{if } -\frac{\pi}{2} \leqslant \phi \leqslant 0, \\ \sqrt{\frac{2-\varepsilon[(-1)^n+1]}{2(1-\varepsilon(-1)^n\cos^2(\phi))}}\prod_{k=-1}^{n-1} J_k(\varepsilon) & \text{otherwise.} \end{cases} \tag{31}$$

The subscripts 'd' and 'v' are used above to distinguish between the initial displacement and initial velocity solutions. The derivation for the initial velocity solution is not provided herein, but is similar to the initial displacement solution presented in Appendix A. The solutions are in an implicit form because ϕ is treated as the independent variable while $t(\phi)$ and $a(\phi)$ are the dependent variables. When $\phi \geqslant \pi/2$, Eq. (27) cannot be solved explicitly for ϕ as it is a transcendental equation in ϕ. Similarly, Eq. (30) is transcendental also for $\phi \geqslant 0$.

When $0 \leqslant \phi \leqslant \pi/2$ or $0 \leqslant t \leqslant \pi/2\sqrt{1-\varepsilon}$, the initial displacement problem (Eqs. (24) and (23)) become

$$x(t) = \cos(t\sqrt{1-\varepsilon}). \tag{32}$$

When $-\pi/2 \leqslant \phi \leqslant 0$ or $0 \leqslant t \leqslant \pi/2\sqrt{1+\varepsilon}$, the initial velocity problem (Eqs. (24) and (29)) become

$$x(t) = \frac{1}{\sqrt{1+\varepsilon}} \sin(t\sqrt{1+\varepsilon}). \tag{33}$$

This simply means the control law has not yet switched the variable stiffness device.

Although the solution obtained above is exact, it is not easily computable, and hence an approximate solution is desired, where comparison can be made to the exact solution as needed.

5.2. An approximate solution

Over a long time period when $t \gg \pi/2\sqrt{1-\varepsilon}$ or $n(\phi) \gg 1$, for the initial displacement problem, the solution can be approximated (see Appendix B for detail) by

$$x(t) \approx \mathrm{e}^{\sqrt{1-\varepsilon}\,\ln(\alpha)/\pi\left(1+\sqrt{\alpha}\right)t} \cos\left[\frac{2\sqrt{1-\varepsilon}}{1+\sqrt{\alpha}}\, t + \theta_d\right], \tag{34}$$

where θ_d is a phase correction term and all other parameters as previously defined. Setting Eqs. (32) and (34) equal at $t = \pi/2\sqrt{1-\varepsilon}$, which corresponds to the first stiffness switch, results in

$$\theta_d = \frac{\pi}{2}\left(\frac{\sqrt{\alpha}-1}{\sqrt{\alpha}+1}\right). \tag{35}$$

This point-matching technique corrects the phase of Eq. (34), so it matches the phase of Eq. (32).

Similarly, an approximate explicit solution for the initial velocity problem can be derived, also by considering the long-term behavior of the system. The approximate solution is

$$x(t) \approx \begin{cases} \frac{1}{\sqrt{1+\varepsilon}} \sin(t\sqrt{1+\varepsilon}) & \text{if } t < t_1, \\ \frac{1}{\sqrt{1+\varepsilon}} \cos(t\sqrt{1-\varepsilon} + \theta_v) & \text{if } t_1 \leqslant t < t_2, \\ \mathrm{e}^{\sqrt{1-\varepsilon}\,\ln(\alpha)/\pi(1+\sqrt{\alpha})t} \sin\left[\frac{2\sqrt{1-\varepsilon}}{1+\sqrt{\alpha}}\, t\right] & \text{otherwise,} \end{cases} \tag{36}$$

where $t_1 = \pi/2\sqrt{1+\varepsilon}$ and $t_2 = \pi(1+\sqrt{\alpha})/2\sqrt{1-\varepsilon}$ are the first and second switching times for the controller, respectively. The first two expressions of Eq. (36) are exact while the last expression is approximate. The middle expression of Eq. (36) is making use of Eq. (32) with a phase correction. Again, by point matching at the switching times, it can be shown that

$$\theta_v = -\frac{\pi}{2}\sqrt{\alpha} \tag{37}$$

and the last expression requires no phase correction. The rationale for point matching the middle equation is because the first switching time occurs close to $t = 0$, which invalidates the long term behavior assumption.

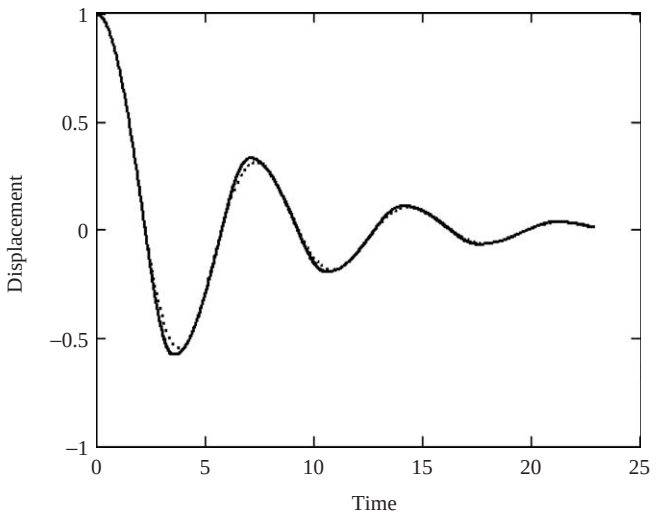

Fig. 1. Comparison of displacement for simulated, implicit, and explicit solutions $\varepsilon = 0.5$. Exact solution (——), approximate solution (.....).

5.3. Time response comparisons

With both the exact and approximate solutions developed, comparisons can now be made of the system solution (Eq. (20)) for the initial displacement problem using three approaches: (1) the simulated solution by an adaptive Runge–Kutta method, (2) the exact implicit solution (Eq. (24)), and (3) the explicit approximate solution (Eqs. (32), (34), and (35)). Similar comparisons can be made for the initial velocity problem, but are omitted for brevity.

No difference was seen between the simulated solution and the exact implicit solution as expected. The approximate explicit solution was found to be a reasonable approximation of the exact implicit solution. Figs. 1 and 2 show the time–response plots comparing the three solutions for two settings of ε. As can be seen in Fig. 1, the approximate solution seems to match the exact solution in terms of phase and frequency, but undershoots the exact solution. In Fig. 2, the undershoot becomes worse for larger values of ε and appears to be greatest in the first period of the response. In later periods, the approximate solution seems closer to the exact solution. This is consistent as the approximate solution was developed for long-time behavior of the system.

5.4. Approximate equivalent viscous damping

A technique commonly used in the literature is to relate the exact system damping to an equivalent viscous damper. Using the results from above, a similar comparison can now be made between the actively controlled variable stiffness device and an equivalent viscous damper system.

The second-order viscously damped system

$$\ddot{x} + 2\zeta\omega_n\dot{x} + \omega_n^2 x = 0 \tag{38}$$

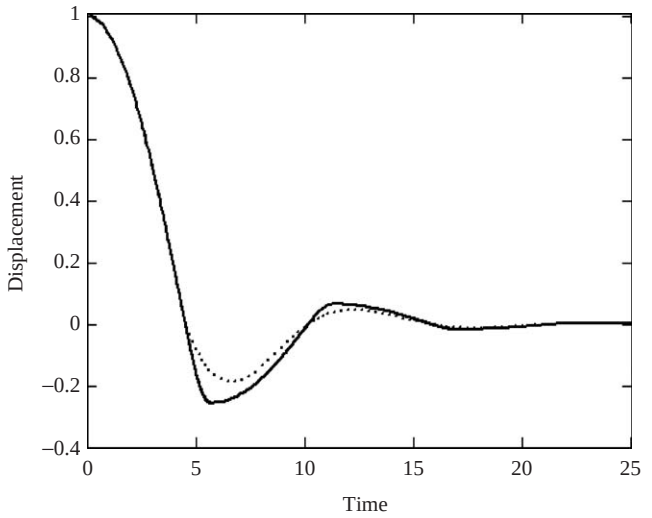

Fig. 2. Comparison of displacement for simulated, implicit, and explicit solutions $\varepsilon = 0.877$. Exact solution (——), approximate solution (.....).

with initial conditions $x(0) = d_0$ and $\dot{x}(0) = v_0$ has the underdamped solution:

$$x(t) = \frac{\sqrt{d_0^2\omega_d^2 + (\dot{x}_0 + \zeta\omega_n x_0)^2}}{\omega_d} \, e^{-\zeta\omega_n t} \cos\left[\omega_d t - \tan^{-1}\left(\frac{v_0 + d_0\zeta\omega_n}{d_0\omega_d}\right)\right], \tag{39}$$

where

$$\omega_d = \omega_n\sqrt{1-\zeta^2}, \tag{40}$$

ζ is the damping ratio, and ω_n is the natural frequency of the system. Eqs. (34) and (39) or Eqs. (36) and (39) can be used to estimate an equivalent viscous damping ratio and natural frequency for the variable stiffness device, valid for the long-term behavior (i.e. $t \gg 1$). The results are

$$\zeta_{\text{eq}} = \frac{|\ln(\alpha)|}{\sqrt{4\pi^2 + \ln(\alpha)^2}}, \tag{41}$$

$$\omega_{n_{\text{eq}}} = \frac{\sqrt{1-\varepsilon}\sqrt{4\pi^2 + \ln(\alpha)^2}}{\pi(1+\sqrt{\alpha})}. \tag{42}$$

Fig. 3 is a plot of Eqs. (41) and (42). As $\varepsilon \to 0$, $\zeta_{\text{eq}} \to 0$ and $\omega_{n_{\text{eq}}} \to 1$. This matches the expected behavior of a simple linear oscillator. As $\varepsilon \to 1$, $\zeta_{\text{eq}} \to 1$ and $\omega_{n_{\text{eq}}} \to 0$, and the system no longer oscillates. Equivalently, Fig. 3 could have been plotted versus α, making use of Eq. (22).

Eq. (41) can be shown to match the theoretical damping ratio Douay and Hagood [4] calculated using an energy method by using Eqs. (9), (10), (2), and (22). Graphing the damping coefficient $\zeta_{\text{eq}}\omega_{n_{\text{eq}}}$ with respect to ε results in a graph that matches the damping ratio plot created by Onoda

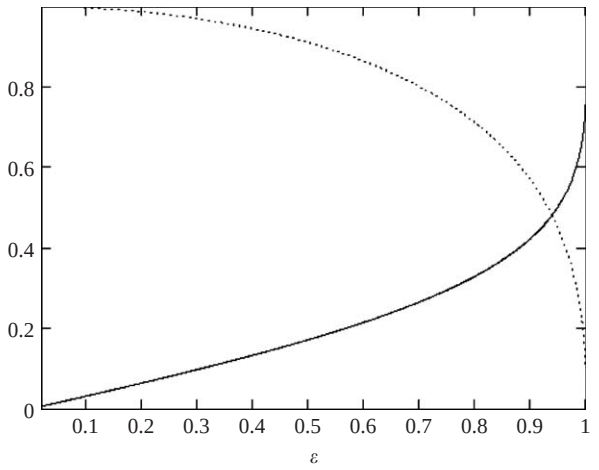

Fig. 3. Equivalent damping and natural frequency of the variable stiffness system. Damping ratio (——), natural frequency (.....).

et al. [5]. The damping coefficient is approximately maximized when $\varepsilon = 0.877$. Referring to Table 1 shows that MREs will potentially provide the best system response for the simple control law used.

6. Conclusions

The literature was surveyed to understand how much stiffness variation was possible in variable stiffness devices currently being developed. Next, a rough understanding of potential performance of the different devices was studied using a sdof problem. While the sdof problem is well documented in the literature, no exact solution to the problem seems to exist. Becaus e the exact solution is in implicit form, an approximate explicit solution was derived directly from the exact solution. The approximate solution was shown to be an excellent approximation of the exact solution. The approximate solution was used to estimate an equivalent viscous damping ratio and an equivalent natural frequency, which were then used to confirm previous literature results. This work adds a new design tool to the engineer's toolbox to aid in the selection of a variable stiffness device to achieve a desired level of damping in a structure. Work is currently underway to extend the result to semi-active damping devices, and alternative control switching schemes.

Appendix A. Exact solution detail

The method of variation of parameters [28] will be applied to solve Eq. (20) with initial conditions $x(0) = 1$ and $\dot{x}(0) = 0$. When $\varepsilon = 0$, the solution to Eq. (20) is

$$x = a\cos(\phi), \tag{A.1}$$

where $\phi = t + \beta$, both a and β are constants. Then,

$$\dot{x} = -a \sin(\phi). \tag{A.2}$$

When $\varepsilon \neq 0$, a and β are functions of time. Then,

$$\dot{x} = \dot{a} \cos(\phi) - a(1 + \dot{\beta}) \sin(\phi) = -a \sin(\phi) + \dot{a} \cos(\phi) - a\dot{\beta} \sin(\phi) \tag{A.3}$$

and

$$\ddot{x} = -\dot{a} \sin(\phi) - a(1 + \dot{\beta}) \cos(\phi) = -\dot{a} \sin(\phi) - a \cos(\phi) - a\dot{\beta} \cos(\phi). \tag{A.4}$$

To put Eqs. (A.2) and (A.3) in the same form requires

$$\dot{a} \cos(\phi) - a\dot{\beta} \sin(\phi) = 0 \tag{A.5}$$

or

$$\dot{\beta} = \frac{\dot{a} \cos(\phi)}{a \sin(\phi)} = \dot{\phi} - 1. \tag{A.6}$$

Substituting Eqs. (A.1), (A.2) and (A.4) into Eq. (20) results in

$$-\dot{a} \sin(\phi) - a\dot{\beta} \cos(\phi) - \varepsilon \operatorname{sgn}(\sin(2\phi)) = 0. \tag{A.7}$$

Substituting Eq. (A.6) into Eq. (A.7) and simplifying results in

$$\frac{\dot{a}}{a} = -\frac{\varepsilon}{2} |\sin(2\phi)|. \tag{A.8}$$

Substituting Eq. (A.8) into Eq. (A.6) and simplifying results in

$$\dot{\phi} = -\frac{\varepsilon}{2}(1 + \cos(2\phi) \operatorname{sgn}(\sin(2\phi))) \equiv f(\phi). \tag{A.9}$$

The initial conditions of Eqs. (A.8) and (A.9) were determined to be $a(0) = 1$ and $\phi(0) = 0$ using Eqs. (A.1) and (A.2). Eq. (A.9) can be solved implicitly as

$$t = \int_0^{\phi} \frac{\mathrm{d}\Phi}{f(\Phi)} \tag{A.10}$$

by realizing that $\operatorname{sgn}(\sin(2\phi))$ changes sign at $\phi_k = k\pi/2$ for $k = 0, 1, \ldots$. Then for $n > 0$,

$$t = \sum_{k=0}^{n-1} \int_{k\pi/2}^{(k+1)\pi/2} \frac{\mathrm{d}\Phi}{((-1)^{k+1}/2)\varepsilon(1 + \cos(2\phi)) + 1} + \int_{n\pi/2}^{\phi} \frac{\mathrm{d}\Phi}{((-1)^{n+1}/2)\varepsilon(1 + \cos(2\phi)) + 1}, \tag{A.11}$$

where $n(\phi) = \operatorname{floor}\left(\frac{2\phi}{\pi}\right)$. For $n = 0$, the summation in Eq. (A.11) does not appear and

$$t = \int_{n\pi/2}^{\phi} \frac{\mathrm{d}\Phi}{((-1)^{n+1}/2)\varepsilon(1 + \cos(2\phi)) + 1}. \tag{A.12}$$

The two integrals in Eq. (A.11) will be evaluated in turn. Applying the transformation $\phi = (k\pi/2) + (v/2)$ to the first integral of Eq. (A.11) produces

$$\int_{k\pi/2}^{(k+1)\pi/2} \frac{\mathrm{d}\Phi}{((-1)^{k+1}/2)\varepsilon(1 + \cos(2\phi)) + 1} = \int_0^{\pi} \frac{\mathrm{d}v}{2 - (-1)^k\varepsilon - \varepsilon \cos(v)} = \frac{\pi}{2\sqrt{1 - (-1)^k\varepsilon}}. \tag{A.13}$$

Applying the transformation $\phi = (n\pi/2) + (v/2)$ to the second integral of Eq. (A.11) produces

$$\int_{n\pi/2}^{\phi} \frac{\mathrm{d}\Phi}{\frac{(-1)^{n+1}}{2}\varepsilon(1+\cos(2\phi))+1} = \int_0^{2\phi-n\pi} \frac{\mathrm{d}v}{2-\varepsilon(-1)^n-\varepsilon\cos v}$$
$$= \frac{1}{\sqrt{1-(-1)^n\varepsilon}} \tan^{-1}\left(\sqrt{\frac{2-\varepsilon((-1)^n-1)}{2-\varepsilon((-1)^n+1)}}\tan\left(\phi-\frac{n\pi}{2}\right)\right). \quad \text{(A.14)}$$

Then Eqs. (A.11) and (A.12) becomes Eq. (27).

Next, Eq. (A.9) will be solved by observing that $\mathrm{d}t = \mathrm{d}\phi/f(\phi)$ and substituting into Eq. (A.9) resulting in

$$\int_0^t \frac{\mathrm{d}a}{a} = -\frac{\varepsilon}{2}\int_0^{\phi} \frac{|\sin(2\Phi)|\,\mathrm{d}\Phi}{f(\Phi)}. \quad \text{(A.15)}$$

Recalling $\mathrm{sgn}(\sin(2\phi))$ changes sign at $\phi_k = k\pi/2$ for $k = 0, 1, \ldots$, when $n > 0$, Eq. (A.15) becomes

$$\ln(a) = -\frac{\varepsilon}{2}\sum_{k=0}^{n-1}\int_{k\pi/2}^{(k+1)\pi/2} \frac{\sin(2\Phi)\,\mathrm{d}\Phi}{-\frac{\varepsilon}{2}(1+\cos(2\Phi)+(-1)^k)}$$
$$-\frac{\varepsilon}{2}\int_{n\pi/2}^{\phi} \frac{\sin(2\Phi)\,\mathrm{d}\Phi}{-\frac{\varepsilon}{2}(1+\cos(2\Phi)+(-1)^n)}. \quad \text{(A.16)}$$

For $n = 0$,

$$\ln(a) = -\frac{\varepsilon}{2}\int_{n\pi/2}^{\phi} \frac{\sin(2\Phi)\,\mathrm{d}\Phi}{-(\varepsilon/2)(1+\cos(2\Phi)+(-1)^n)}. \quad \text{(A.17)}$$

Letting $\phi = (k\pi/2) + (v/2)$, the first integral of Eq. (A.16) evaluates as

$$\int_{k\pi/2}^{(k+1)\pi/2} \frac{\sin(2\Phi)\,\mathrm{d}\Phi}{-\frac{\varepsilon}{2}(1+\cos(2\Phi)+(-1)^k)} = \int_0^{\pi} \frac{\sin v\,\mathrm{d}v}{2-\varepsilon(-1)^K-\varepsilon\cos v}$$
$$= \ln\left(\frac{2-\varepsilon[(-1)^k-1]}{2-\varepsilon[(-1)^k+1]}\right)^{1/\varepsilon}. \quad \text{(A.18)}$$

Letting $\phi = (n\pi/2) + (v/2)$, the second integral of Eq. (A.16) evaluates as

$$\int_{n\pi/2}^{\phi} \frac{\sin(2\Phi)\,\mathrm{d}\Phi}{-\frac{\varepsilon}{2}(1+\cos(2\Phi)+(-1)^n)} = \int_0^{2\phi-n\pi} \frac{\sin v\,\mathrm{d}v}{2-\varepsilon(-1)^n-\varepsilon\cos v}$$
$$= \ln\left(\frac{2-\varepsilon(-1)^n[1+\cos(2\phi)]}{2-\varepsilon[(-1)^n+1]}\right)^{1/\varepsilon}. \quad \text{(A.19)}$$

Then, Eq. (A.16) becomes

$$\ln(a) = \sum_{k=0}^{n-1} \ln\left(\frac{2-\varepsilon[(-1)^k-1]}{2-\varepsilon[(-1)^k+1]}\right)^{-1/2} + \ln\left(\frac{2-\varepsilon(-1)^n[1+\cos(2\phi)]}{2-\varepsilon[(-1)^n+1]}\right)^{-1/2} \quad \text{(A.20)}$$

and Eq. (A.17) becomes

$$\ln(a) = \ln\left(\frac{2-\varepsilon(-1)^n[1+\cos(2\phi)]}{2-\varepsilon[(-1)^n+1]}\right)^{-1/2}, \tag{A.21}$$

resulting in the solution shown in Eq. (28).

Appendix B. approximate explicit solution detail

For $\phi > \frac{\pi}{2}$, Eq. (27) can be rewritten as

$$t(\phi) = \frac{1}{\sqrt{1-\varepsilon}}\left[\frac{n\pi}{4}(1+\sqrt{\alpha}) + \begin{cases} \tan^{-1}\left(\frac{1}{\sqrt{1-\varepsilon}}\tan(\phi)\right) & \text{if } n(\phi) \text{ is even,} \\ -1-\alpha\tan^{-1}(\sqrt{1+\varepsilon}\cot(\phi)) & \text{if } n(\phi) \text{ is odd} \end{cases}\right]. \tag{B.1}$$

When $n(\phi) \gg 1$,

$$t(\phi) \approx \frac{n\pi}{4}\frac{(1+\sqrt{\alpha})}{\sqrt{1-\varepsilon}}. \tag{B.2}$$

Approximating

$$n(\phi) \approx \frac{2\phi}{\pi} \tag{B.3}$$

and solving Eq. (B.2) for $\phi(t)$ results in

$$\phi \approx \frac{2\sqrt{1-\varepsilon}}{1+\sqrt{\alpha}}\, t. \tag{B.4}$$

Next, Eq. (28) is rewritten as

$$a(\phi) = \alpha^{n(\phi)/4}\frac{\sqrt{1-\varepsilon}}{\sqrt{1-\varepsilon\cos^2\phi}}\begin{cases} 1 & \text{if } n(\phi) \text{ is even,} \\ (1-\varepsilon^2)^{1/4} & \text{if } n(\phi) \text{ is odd.} \end{cases} \tag{B.5}$$

Again assuming $n(\phi) \gg 1$ and using Eqs. (B.3) and (B.4) results in

$$a(\phi) \approx \alpha^{n(\phi)/4} \approx \alpha^{\phi/2\pi} \approx \alpha^{(2\sqrt{1-\varepsilon})/(\pi(1+\sqrt{\alpha}))t}. \tag{B.6}$$

Substituting Eqs. (B.4) and (B.6) into Eq. (24) produces Eq. (34).

References

[1] N. Jalili, A comparative study and analysis of semi-active vibration-control systems, *Journal of Vibration and Acoustics* 124 (4) (2002) 593–605.

[2] J. Sun, M. Jolly, M. Norris, Passive, adaptive and active tuned vibration absorbers—a survey, *50th anniversary of the design engineering division, A Special Combined Issue of the Journal of Mechanical Design and the Journal of Vibration and Acoustics* 117 (3B) (1995) 234–242.

[3] G. Leitmann, Semiactive control for vibration attenuation, *Journal of Intelligent Material Systems and Structures* 5 (1994) 841–846.

[4] A. Douay, N. Hagood, Evaluation of optimal variable stiffness feedback control authority stability, feasibility and implementation, in: *Proceedings of the Fourth International Conference on Adaptive Structures*, 1993, pp. 388–404.
[5] J. Onoda, T. Sano, K. Kamiyama, Active, passive and semi-active vibration suppression by stiffness variation, *AIAA Journal* 30 (12) (1992) 2922–2929.
[6] T. Kobs, J. Sun, A non-linear variable stiffness feedback control with tuning range and rate saturation, *Journal of Sound and Vibration* 205 (2) (1997) 243–249.
[7] http://smart.tamu.edu/overview/overview.html
[8] D. Lagoudas, J. Mayes, M. Khan, Simplified shape memory alloy (SMA) material model for vibration isolation, in: V. Rao (Ed.), *Proceedings of the SPIE*, *vol.* 4326, *Smart Structures and Materials 2001: Modeling*, *Signal Processing*, *and Control in Smart Structures*, 2001, pp. 452–461.
[9] M. Khan, D. Lagoudas, Modeling of shape memory alloy pseudoelastic spring elements using Preisach model for passive vibration isolation, in: V. Rao (Ed.), *Proceedings of the SPIE*, *vol.* 4693, *Smart Structures and Materials 2002: Modeling*, *Signal Processing*, *and Control*, 2002, pp. 336–347.
[10] D. Grant, V. Hayward, Design of shape memory alloy actuator with high strain and variable structure control, in: *Proceedings of the* 1995 *IEEE International Conference on Robotics and Automation*, 1995, pp. 2305–2312.
[11] K. Williams, G. Chiu, R. Bernhard, Adaptive-passive absorbers using shape-memory alloys, *Journal of Sound and Vibration* 249 (5) (2002) 835–848.
[12] J. Ginder, M. Nichols, L. Elie, J. Tardiff, Magnetorheological elastomers: properties and applications, in: M. Wuttig (Ed.), *Proceedings of the SPIE*, *vol.* 3675, *Smart Structures and Materials 1999: Smart Materials Technologies*, *SPIE-International Society for Optical Engineering*, 1999, pp. 131–138.
[13] J. Carlson, M. Jolly, MR fluid, foam and elastomer devices, *Mechatronics* 10 (4–5) (2000) 555–569.
[14] G. Zhou, Shear properties of a magnetorheological elastomer, *Smart Materials and Structures* 12 (2003) 139–146.
[15] A.-M. Albanese, K. Cunefare, Properties of a magnetorheological semiactive vibration absorber, in: G. Agnes, K.-W. Wang (Eds.), *Proceedings of the SPIE*, *vol.* 5052, *Smart Structures and Materials 2003: Damping and Isolation*, 2003, pp. 36–43.
[16] A.-M. Albanese, K. Cunefare, *Properties of a Magnetorheological Semiactive Vibration Absorber*, 2003.
[17] G. Lesieutre, Vibration damping and control using shunted piezoelectric materials, *Shock and Vibration Digest* 30 (3) (1998) 187.
[18] C. Richard, D. Guyomar, D. Audigier, G. Ching, Semi-passive damping using continuous switching of a piezoelectric device, in: H.T. Tupper (Ed.), *Proceedings of the SPIE, vol.* 3672, *Smart Structures and Materials 1999: Passive Damping and Isolation*, 1999, pp. 104–111.
[19] L. Corr, W. Clark, Energy dissipation analysis of piezoceramic semi-active vibration control, *Journal of Intelligent Material Systems and Structures* 12 (11) (2001) 729–736.
[20] L. Corr, W. Clark, Comparison of low-frequency piezoelectric switching shunt techniques for structural damping, *Smart Materials and Structures* 11 (3) (2002) 370–376.
[21] W. Clark, Vibration control with state-switched piezoelectric materials, *Journal of Intelligent Material Systems and Structures* 11 (4) (1999) 263–271.
[22] C. Davis, G. Lesieutre, An actively tuned solid-state vibration absorber using capacitive shunting of piezoelectric stiffness, *Journal of Sound and Vibration* 232 (3) (2000) 601–617.
[23] A. Ramaratnam, N. Jalili, M. Grier, Piezoelectric vibration suppression of translational flexible beams using switched stiffness, in: *Proceedings of 2003 IMECE*, ASME, Washington DC, 2003.
[24] J. Onoda, K. Minesugi, Semiactive vibration suppression by variable-damping members, *AIAA Journal* 34 (2) (1996) 340–347.
[25] S. Kelso, R. Blankinship, B. Henderson, Precision controlled actuation and vibration isolation utilizing magnetorheological (MR) fluid technology, in: *IAA Space* 2001 *Conference*, 2001.
[26] M. Franchek, M. Ryan, R. Bernhard, Adaptive passive vibration control, *Journal of Sound and Vibration* 189 (5) (1995) 565–585.
[27] P. Walsh, J. Lamancusa, A variable stiffness vibration absorber for minimization of transient vibrations, *Journal of Sound and Vibration* 158 (2) (1992) 195–211.
[28] R. Wylie, L. Barrett, *Advanced Engineering Mathematics*, sixth ed., McGraw-Hill, New York, 1995.